

## Development of Digital Wind Tunnel as a Subsystem of JAXA Digital/Analog Hybrid Wind Tunnel

Keiichi Murakami<sup>1)</sup>  
Atsushi Hashimoto<sup>1)</sup>  
Manabu Hishida<sup>2)</sup>  
Paulus R. Lahur<sup>3)</sup>  
Akira Kunieda<sup>4)</sup>  
Shigeya Watanabe<sup>5)</sup>

1) Numerical Analysis Group, Aerospace Research and Development Directorate  
Japan Aerospace Exploration Agency (JAXA)  
7-44-1, Jindaiji Higashi-machi, Chofu-shi, Tokyo, 182-8522  
Japan  
murakami.keiichi@jaxa.jp  
hashimoto.atsushi@jaxa.jp

2) Numerical Analysis Group, Aerospace Technology Dept., Engineering Solution Div.  
Ryoyu Systems Co., Ltd.  
6-19 Oye-cho, Minato-Ku, Nagoya, 455-0024  
Japan  
MANABU\_HISHIDA@mail.ryoyu.co.jp

3) Meshing Technical Development Dept.  
Research Center of Computational Mechanics, Inc. (RCCM)  
Togoshi NI-Bldg., 1-7-1, Togoshi, Shinagawa-ku, Tokyo, 142-0041  
Japan  
lahur@oi.rccm.co.jp

4) Systems Div. 2, Systems Development Services Unit 2  
Computer Engineering & Consulting, Ltd. (CEC)  
Shirakawa 8th Bldg., 1-10-29, Marunouchi, Naka-ku, Nagoya, 460-0002  
Japan  
cecakira@chofu.jaxa.jp

5) Wind Tunnel Technology Center, Aerospace Research and Development Directorate  
Japan Aerospace Exploration Agency (JAXA)  
7-44-1, Jindaiji Higashi-machi, Chofu-shi, Tokyo, 182-8522  
Japan  
watanabe.shigeya@jaxa.jp

### Abstract

Japan Aerospace Exploration Agency (JAXA) is developing a practical Experimental Fluid Dynamics and Computational Fluid Dynamics (EFD/CFD) integration system called the Digital/Analog Hybrid Wind Tunnel (DAHWIN), where 'Digital' and 'Analog' denote CFD and EFD (or wind tunnel), respectively. The aim of this system is to improve effectiveness, accuracy, and reliability of wind tunnel tests by jointly utilizing CFD as well

as some advanced techniques for the EFD/CFD integration. For the development of the Digital Wind Tunnel (DWT), both features of high-speed performance and high degree of accuracy must be accomplished simultaneously for realizing the timely use of the DAHWIN system and high-fidelity wind tunnel data corrections. In this paper, several functions of the DWT and a newly-developed fast CFD routine for the DWT are introduced.

Key words: digital wind tunnel, computational fluid dynamics

## Introduction

One of the main features of the Digital/Analog Hybrid Wind Tunnel [1] named DAHWIN is quasi real-time visualization of CFD and wind tunnel data during the test, so that we can immediately check the measured data comparing with the CFD result. The CFD data is prepared in advance before the testing and huge parametric study of Mach number and angle of attack is necessary. Therefore, we need a fast CFD tools to improve the productivity to integrate the CFD and EFD.

During wind tunnel test campaign, approximately 200 aerodynamic data are obtained every day. The campaign continues for 8 days in general. Therefore, the total 1600 data are obtained in one campaign. Since it is difficult to carry out CFD for all cases with the current high performance computer technologies, we set our target as 1/5 data of them. If we carry out the CFD in 20 days, the required speed is approximately one hour per case. In order to achieve one hour computation time per case, we have newly developed a fast CFD codes.

For the CFD side, the goal is to reduce the simulation cycle time to the order of hours as mentioned above. The essential technique to achieve this is through automatic grid generation. Automatic grid generation is a great improvement over manual grid generation in terms of ease-of-use and time consumed. A process that used to take weeks can be drastically reduced to an hour. Another important goal is the level of solution accuracy. It has to be sufficient enough to predict drag. This capability has been satisfactorily demonstrated in our participation in the 4th Drag Prediction Workshop (DPW4) [2-4], in which participants submitted their computation on a standard transonic aircraft model.

These automatic grid generation and CFD tools are installed into the DWT as a subsystem of the DAHWIN, and are called from several functions of DWT. The aerodynamic coefficients obtained by CFD are stored in the database of DAHWIN with the same format of wind tunnel test data to establish EFD and CFD database.

## Installed CFD tools

For the development of the DWT, both features of high-speed performance and high degree of accuracy must be accomplished simultaneously in order to realize the timely use of the hybrid wind tunnel system and the high-fidelity wind tunnel data corrections. Mainly, a newly-developed fast CFD solver called FaSTAR (FaST Aerodynamic Routine) [5] for unstructured grid is installed in combination with an automatic unstructured grid generator, HexaGrid [6], using the Cartesian grid generation technique.

The grid made by HexaGrid is a hybrid between Cartesian grid and prismatic grid, where the Cartesian grid fills the far-field region and the prismatic grid fills the region around solid surface to resolve boundary layer flow. Cartesian grid was chosen due to its speed in filling computational domain, owing to the fact that it does not follow body surface, a property known as non-body-fitted. HexaGrid uses body surface data in STL (Stereo Lithography) format, which describes the surface as a set of triangles, and achieves grid generation that is tolerant to defects in STL representation. This brings us closer to full automation of the whole simulation process, and may reduce the order of simulation time to a few hours. Using HexaGrid, it is possible to generate a grid with twelve million cells automatically within an hour by a 64-bit PC around a generic civil transport configuration named NASA CRM as shown in Fig. 1.

FaSTAR consists of three parts: pre-processor, flow solver, and post-processor. The pre-processor implements a conversion of grid data format, a decomposition of calculation domain, a computation of cell volume and face area, and a reordering with Cuthill-Mackee. The flow solver compute flows, and the post-process make data for visualization. Governing equation of FaSTAR can be chosen from Euler and RANS. As turbulence model, Spalart-Allmaras, SST models or so were implemented. Accuracy of drag coefficient should be less than 10 counts (1 count means 0.0001 of aerodynamic coefficient) to be used for an industrial vehicle development. The portion of pre-process is relatively high in this code, and this is designed for efficient joint development and maintenance purpose.

Considering the use of the new CFD solver, FaSTAR, in the pretest CFD calculations, target of its calculation speed performance was set to an hour per case for a grid with ten million cells using a hundred CPUs of JAXA Supercomputer System (JSS). Although the FaSTAR is under development at present, its preliminary version has been completed as a RANS solver with two convergence acceleration techniques, that is, the multi-grid technique and GMRES. Incorporating two convergence acceleration techniques will be realized four times faster calculation than before, indicating that the target of calculation speed was accomplished.

For verification and validation of FaSTAR, we carry out several test computations. As preliminary test, the one-dimensional shock tube problems (Sod's problems) are solved. Then, the laminar and turbulent boundary layers are computed. These computational results are found to agree well with theoretical solutions. Since FaSTAR is used for comparison of aerodynamic coefficients with wind tunnel data, accuracy of aerodynamic prediction is important. Therefore, the accuracy of drag prediction with FaSTAR is validated by the DPW4 benchmark problems. The computation result of  $C_p$  distribution on the surface of NASA CRM with FaSTAR is shown in Fig. 1. Although we employ the hexahedra-based grid generated with HexaGrid, the computed drag coefficients generally agree with other results [5].

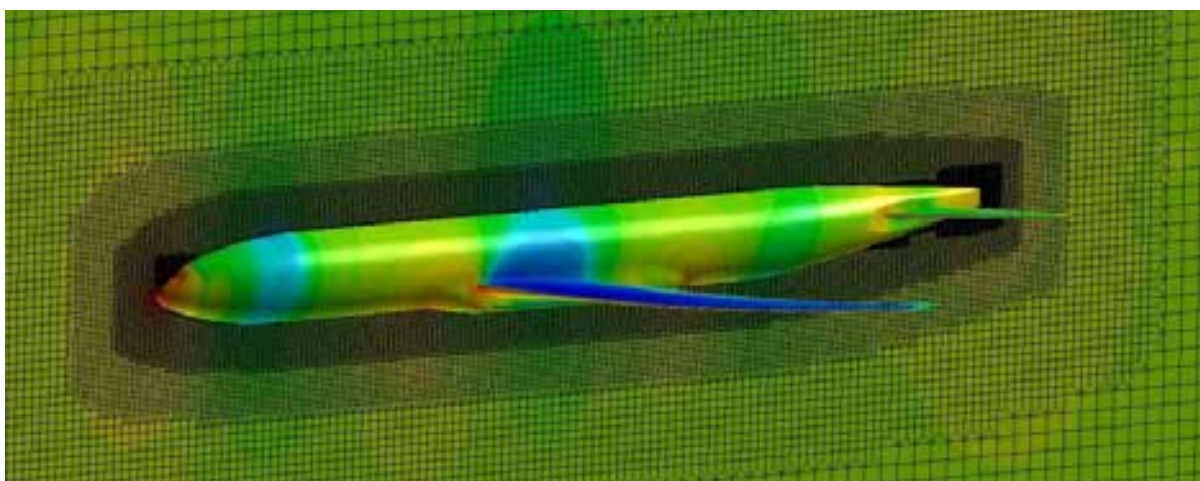


Figure 1. Computational grid and result of  $C_p$  distribution for NASA CRM.

## Parametric CFD

The main function of DWT is a parametric CFD function, which is constructed from automatic workflow of grid generation, CFD calculation on JSS, and storing the results to database. The pretest CFD calculations are performed for the preparation of wind tunnel test with wind tunnel flow conditions of different Mach number, Reynolds number, and angle of attack. The number of pretest CFD cases is supposed to 20 percent of wind tunnel test cases. The results of pretest parametric CFD is used to improve the efficiency as well as the reduction of risk in wind tunnel tests, to make a real time comparison of the experimental data of force/pressure ports data with that of CFD data for checking the validity of the measurement data during the test period, to correct the support interference effect of the wind tunnel data, and so on. The results of pressure distribution on the surface of wind tunnel model by CFD are also compared with that obtained from Pressure-Sensitive Paint (PSP) measurement. In addition, the results of flow vector around the model are compared with that obtained from Particle Image Velocimetry (PIV) measurement.

Using the DWT, it is possible to count the aerodynamic coefficients of each part of a model, which are constructed from STL data of fuselage, wing, nacelle, pylon, model support and so on. Therefore, users can examine the influence of model supports on each part in the pretest CFD calculations. Before manufacturing wind tunnel test models and supports, the DWT can be used to evaluate the effects of the configuration of model support on the flow field around the model. An example of grid generation including two different types of model support, that is, blade-type sting and straight sting, is shown in Fig. 2. Also, corresponding RANS calculation results of  $C_p$  map on surfaces of the model and sting are shown in Fig. 3. The results on grid generation suggest the robustness of HexaGrid while the results of the RANS calculations clearly indicate the model support effect which is seen on the model surface pressure distribution near the junction of the model and

support. Based on these results, the users can choose the best configuration of model support sting without manufacturing several different stings to check the effects of the support configuration during wind tunnel tests.

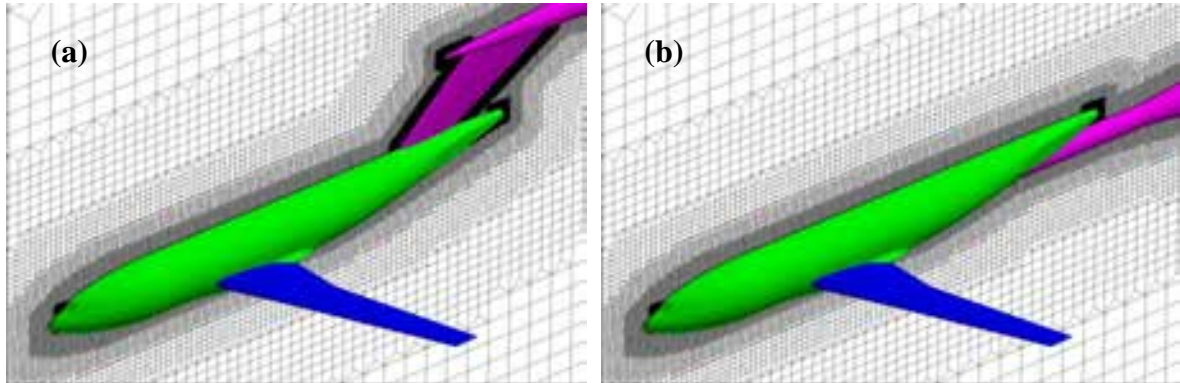


Figure 2. Examples of automatically generated grid including two different model support around the DLR F6-FX2B model; (a) Blade-type sting support, (b) Straight sting support.

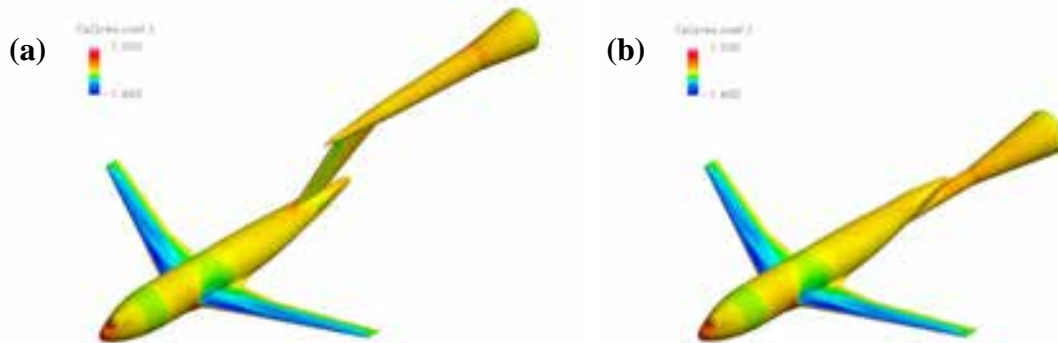
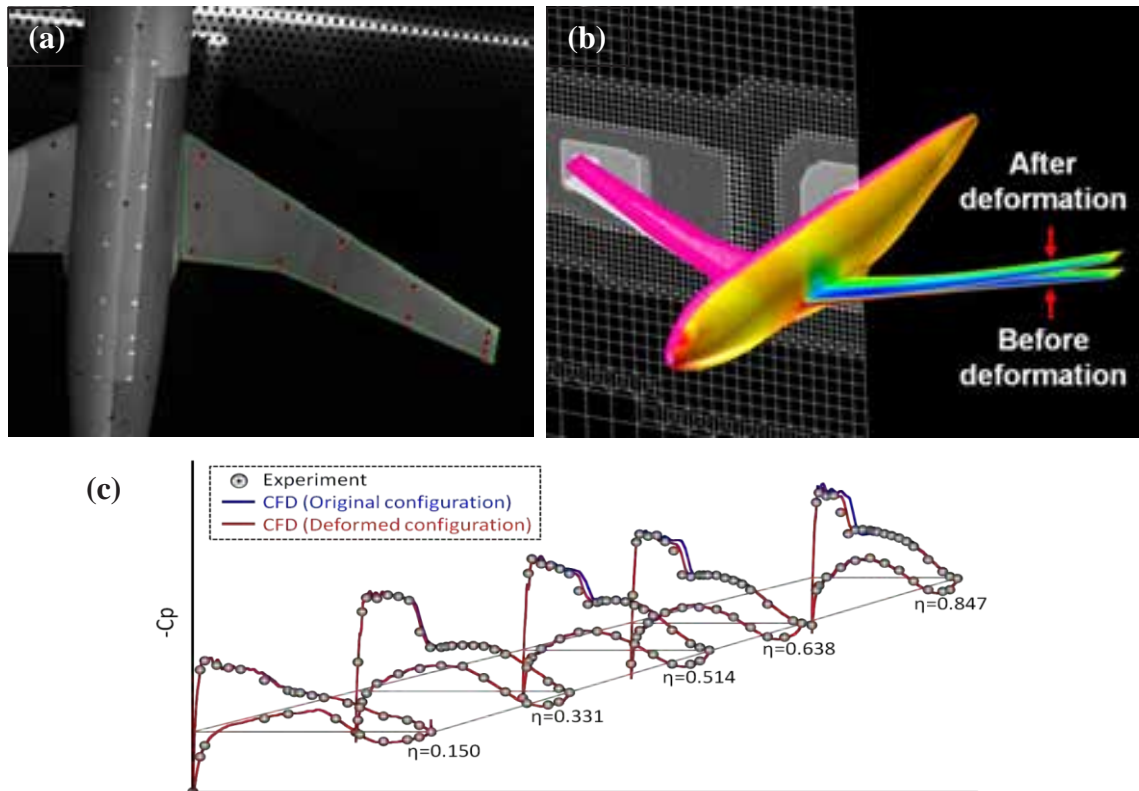


Figure 3. Calculation results of Cp map on surfaces of the DLR F6-FX2B model; (a) Blade-type sting support, (b) Straight sting support.

## Static Model Deformation

During a wind tunnel test, a part of model such as a wing is deformed under the circumstances. The deformation of wing affects the aerodynamic coefficients, and causes the difference between EFD data and CFD calculations. It is possible to take a model deformation into account to CFD calculations using the Static Model Deformation Function of DWT. Users need to obtain displacement data of a deformed model, which are measured at dispersed points on wing surface during wind tunnel test. This function has an algorithm of whole wing deformation with displacement data at discrete points, which is called Z44 model and installed as a default. In addition, the Surface Influence (SI) method is installed as a default algorithm of grid deformation on the assumption that a degree of wing deformation is small. The SI method is one of algebraic schemes for fast grid deformation, and has good prospects of high performance of DWT because of high parallelization ability and easier implementation.

Figure 4 shows an example of the model deformation computation using measurement data. Model deformation measurements were made using stereo photogrammetry with markers as shown in Fig.4 (a). The information for the marker displacement is then used to deform the CFD model surface and volume mesh (Fig. 4(b)). The detail of the numerical technique can be found in [7]. As can be confirmed in Fig. 4 (c), the pressure distribution of CFD shows closer values compared to wind tunnel data if the effect of deformation is taken into account. The process of the present analysis (measurement data acquisition, surface/ volume mesh deformation, and CFD execution) can be made automatically through the DWT system if both measurement/pretest CFD data are available.



**Figure 4. Model deformation computation using measurement data; (a) markers for stereo photogrammetry, (b) CFD model geometry before/after the deformation, (c) comparison of chord-wise static pressure distribution.**

## Fluid-Structure Interaction

The DWT has a function of Fluid-Structure Interaction (FSI) analysis, which can analyze a static aeroelasticity of the main wing. In the present FSI function, a user needs to input the unstructured mesh data for the structural analysis of wing, which is generated by PATRAN for example. The mesh for structural analysis is, in general, different from that for CFD, and the former is coarse in comparison with the later. An appropriate data converter is, therefore, made in order to map the pressure distributions on wing surface, which is obtained by CFD calculation, on the mesh for structural analysis. The structural analysis is executed to deform the wing shape by static load distribution, which is converted from converged CFD calculation result. The NASTARN is used for the structural analysis. The loop of FSI analysis is performed until the degree of deformation and the change on aerodynamic coefficients become small.

Figures 5-7 show an example of FSI calculation. Computational conditions are Mach number of  $M=0.75$ , angle of attack of 1 degree, and Reynolds number of  $Re=1.5 \times 10^6$ . SA turbulence model is employed as turbulence model. It is assumed that the physical properties of a solid wing are Young's modulus of 208GPa and Poisson's ratio of 0.27, which are the same as that of wind tunnel test model. Figure 5 (a) shows the  $C_p$  distributions on wing surface mesh of CFD calculation. Figure 5 (b) shows the mesh and static load mapping for structural calculation. It is also assumed that the wing is only deformable part. In this example, the static balance is achieved after that the FSI loop is iterated three times as shown in Fig. 6 and Table 1. Here,  $C_p$  plots on wing cross section of non-deformed and deformed cases are compared in Fig. 7. In Fig. 7, the experimental data are also plotted with solid circle. The close section is located at 0.638% and 0.847% of wing span length. The computational  $C_p$  distribution becomes closer to experimental results by considering the wing deformation. The influence of wing deformation on  $C_p$  distribution is, however, very small in this example. The reason of that is the assumption of solid wing, which has no laying pipes for pressure measurement ports. The inside structure of wind tunnel test model is more complicate, and does not have simple solid wing. The assumption of solid wing makes the structural model inflexible rather than the actual wind tunnel test model.

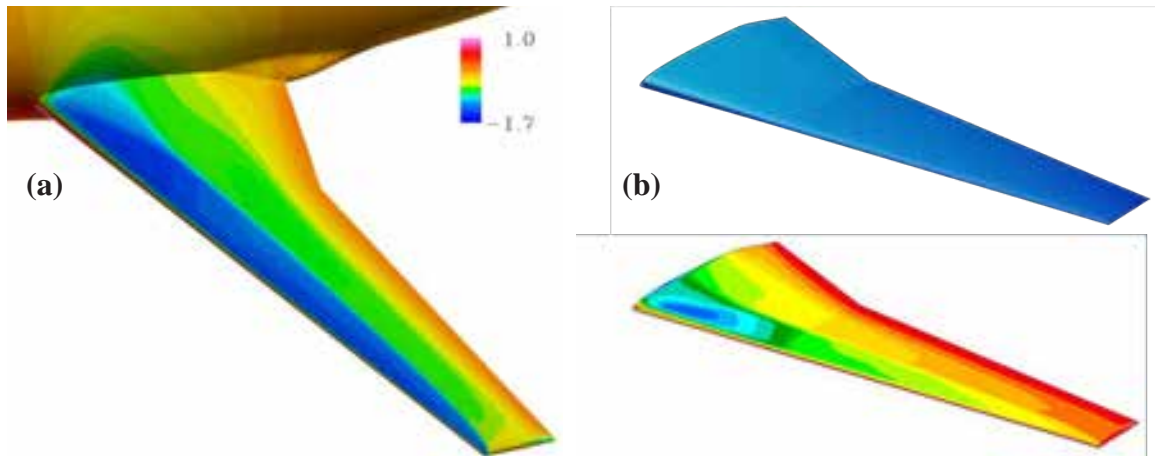


Figure 5. Cp and static load distributions on wing surface; (a) Cp, (b) static load

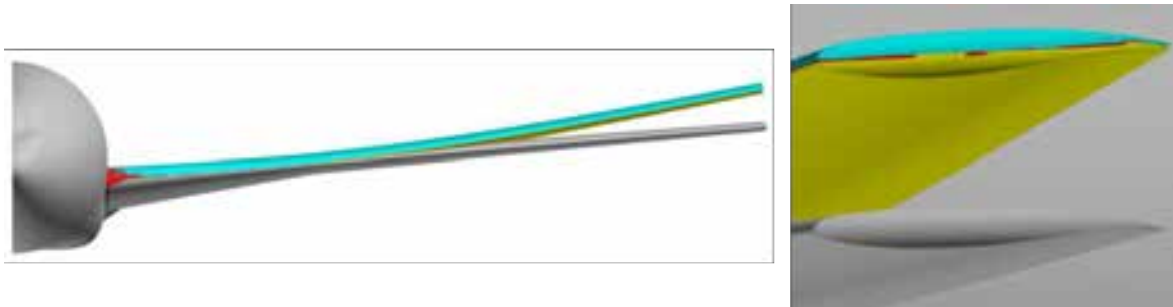


Figure 6. Wing deformation by FSI loop.

Table 1. Aerodynamic coefficient of each FSI loop.

FSI Loop No.	0 (Original)	1	2	3 (Converged)
$C_D$	0.0359	0.0354	0.0354	0.0354
$C_L$	0.5940	0.5867	0.5868	0.5868
$C_m$	-0.1267	-0.1244	-0.1244	-0.1244

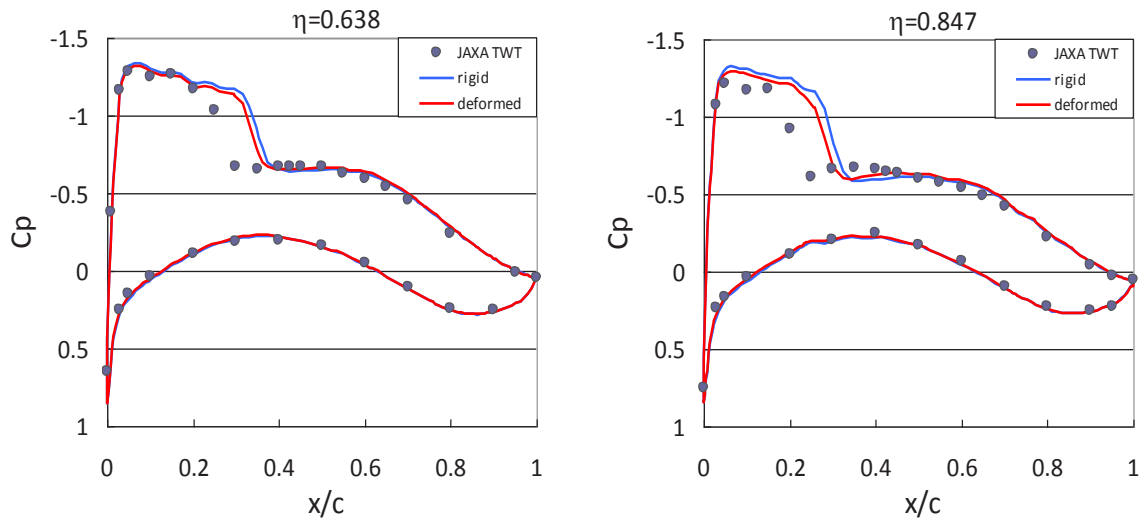


Figure 7.  $C_p$  plots of wing cross sections.

## Summary

The CFD tools, which are installed into the DWT, were presented. The functions of parametric CFD, measured static model deformation, and fluid-structure interaction calculation were also presented. We are improving these tools and functions day by day toward to the completion of DAHWIN system, which is scheduled on the end of this fiscal year.

The future works on CFD tools are modeling of roughness on the wing surface, structural calculation parameters, and porous wall of wind tunnel, for example. These modeling will close computation aerodynamic coefficients to experimental that. Although the EFD/CFD integration technology has not been matured, we believe that a fast and accurate CFD code accelerates the integration of them.

## References

- [1] S. Watanabe, S. Kuchi-ishi, K. Murakami, A. Hashimoto, H. Kato, T. Yamashita, K. Yasue, K. Imagawa, and K. Nakakita: Development Status of a Prototype System for EFD/CFD Integration, 47th Applied Aerodynamics Symposium, FP54-2012, 2012.
- [2] A. Hashimoto, K. Murakami, T. Aoyama, and P. R. Lahur: Lift and Drag Prediction Using Automatic Hexahedra Grid Generation Method, AIAA paper 2009-1365, 2009.
- [3] A. Hashimoto, K. Murakami, T. Aoyama, K. Yamamoto, M. Murayama, and P. R. Lahur: Drag Prediction on NASA CRM using Automatic Hexahedra Grid Generation, AIAA Paper 2010-1417, 2010.
- [4] A. Hashimoto, P. R. Lahur, K. Murakami, and T. Aoyama: Validation of fully automatic grid generation method on aircraft drag prediction. AIAA Paper 2010-4669, 2010.
- [5] A. Hashimoto, K. Ishiko, M. Hishida, K. Murakami, P. R. Lahur, M. Sakashita, and T. Aoyama: Toward the Fastest Unstructured CFD Code 'FaSTAR.' AIAA Paper 2012-1075, 2012.
- [6] P. R. Lahur: Automatic Hexahedra Grid Generation Method for Component-based Surface Geometry, AIAA paper 2005-5242, 2005.
- [7] K. Yasue, S. Kuchi-ishi, A. Hashimoto, K. Murakami, H. Kato, K. Nakakita, S. Watanabe, and M. Hishida: High-Fidelity CFD Simulation of a Wind Tunnel Model Using Model Deformation Data, Proceedings of 15th International Forum on Aeroelasticity and Structural Dynamics, 2010.